Available online at www.sciencedirect.com
ScienceDirect
Bioorganic & Medicinal Chemistry 14 (2006) 6859–6867
Bioorganic & Medicinal Chemistry

# Molecular modeling of the non-covalent binding of the dietary tomato carotenoids lycopene and lycophyll, and selected oxidative metabolites with 5-lipoxygenase

Eszter Hazai,[a] Zsolt Bikádi,[a] Ferenc Zsila[b] and Samuel F. Lockwood[c,*]

[a]*Virtua Drug, Ltd, H-1015 Budapest, Csalogány st. 4, Hungary*
[b]*H-2092 Budakeszi, Rózsa st. 18, Hungary*
[c]*Cardax Pharmaceuticals, Inc., 99-193 Aiea Heights Drive, Suite 400, Aiea, HI 96701, USA*

Received 23 May 2006; revised 13 June 2006; accepted 19 June 2006
Available online 11 July 2006

**Abstract**—Numerous studies on human prostate cancer cell lines indicate a role for arachidonic acid (AA) and its oxidative metabolites in prostate cancer proliferation. The metabolism of AA by either the cyclooxygenase (COX) or the lipoxygenase (LOX) pathways generates eicosanoids involved in tumor promotion, progression, and metastasis. In particular, products of the 5-LOX pathway (including 5-HETE and 5-oxo-EET) have been implicated as potential 'survival factors' that may confer escape after androgen withdrawal therapy through fatty-acid (i.e., AA) drive. Potent natural dietary antioxidant compounds such as lycopene and lycophyll, with tissue tropism for human prostate, have been shown to be effective in ameliorating generalized oxidative stress at the DNA level. Suppressing the 5-LOX axis pharmacologically is also a promising avenue for intervention in human patients. The recently recognized direct interaction of the astaxanthin-based soft-drug Cardax™ to human 5-LOX with molecular modeling, and the downregulation of both 5-HETE and 5-oxo-EET in vivo in a murine peritonitis model, suggest that other important dietary carotenoids may share this enzyme regulatory feature. In the current study, the acyclic tomato carotene lycopene (in all-*trans* and 5-*cis* isomeric configurations) and its natural dihydroxy analog lycophyll (also present in tomato fruit) were subjected to molecular modeling calculations in order to investigate their predicted binding interaction(s) with human 5-LOX. Two bioactive oxidative metabolites of lycopene (4-methyl-8-oxo-2,4,6-nonatrienal and 2,7,11-trimethyl-tetradecahexaene-1,14-dial) were also investigated. A homology model of 5-LOX was constructed using 8-LOX and 15-LOX structures as templates. The model was validated by calculating the binding energy of Cardax™ to 5-LOX, which was demonstrated to be in good agreement with the published experimental data. Blind docking calculations were carried out in order to explore the possible binding sites of the carotenoids on 5-LOX, followed by focused docking to more accurately calculate the predicted energy of binding. Lycopene and lycophyll were predicted to bind with high affinity in the superficial cleft at the interface of the β-barrel and the catalytic domain of 5-LOX (the 'cleavage site'). Carotenoid binding at this cleavage site provides the structural rationale by which polyenic compounds could modify the 5-LOX enzymatic function via an allosteric mechanism, or by radical scavenging in proximity to the active center. In addition, the two bioactive metabolites of lycopene were predicted to bind to the catalytic site with high affinity—therefore suggesting potential direct competitive inhibition of 5-LOX activity that should be shared by both lycopene and lycophyll after in vivo supplementation, particularly in the case of the dial metabolite.


## 1. Introduction

Carotenoids comprise a class of natural mostly fat-soluble pigments of more than 750 structurally distinct compounds (exclusive of *cis* and *trans* isomers) which are found in numerous fruits and vegetables, as well as fish, crustaceans, and birds.[1,2] Tomato fruit (*Lycopersicum esculentum* Mill) contains a related set of acyclic C40 carotenoids, the carotene lycopene and the xanthophylls, lycoxanthin and lycophyll, with lycopene in predominant abundance and responsible for the fruit's deep red color. The central carbon chain of alternating single and double bonds in the lycopene series is 11 conjugated bonds in length, and confers the greatest singlet oxygen quenching ability among tested carotenoids.[3] The consumption

*Keywords*: 5-HETE; 5-oxo-EET; 5-Lipoxygenase; 5-LOX; Astaxanthin; Blind docking; Homology modeling; Lycopene; Lycophyll; Oxidative metabolites.
* Corresponding author. Tel.: +808 220 9168; fax: +808 237 5901; e-mail: slockwood@cardaxpharma.com

0968-0896/$ - see front matter © 2006 Elsevier Ltd. All rights reserved.
doi:10.1016/j.bmc.2006.06.045

of a diet rich in carotenoids—in particular lycopene—has been epidemiologically correlated with a lower risk for several chronic diseases, including prostate cancer.[4–6] Mounting evidence in model animal systems and in humans surrounding the consumption of tomato fruit and tomato-derived products, either as whole-food interventions or supplements,[7–9] suggests promise for tomato-derived phytochemicals for the chemoprevention and/or chemotherapy of prostate malignancy.[10]

The protective effects of tomato products in prostate and other pathology have recently been more directly linked to the non-provitamin A carotenoid lycopene.[11,12] Together with α- and β-carotene (also pro-vitamin A carotenes), lycopene is a prominent member of the dietary carotene group, which includes those carotenoids composed only of carbon and hydrogen atoms. As an antioxidant, the highly unsaturated lycopene is about twice as effective as its cyclic isomer β-carotene. The all-*trans* form of lycopene predominates in nature and also comprises the vast majority of geometric isomers in human food sources (up to 90% in tomato products).[13] However, *cis* isomeric forms of lycopene are the predominant carotenoids in human blood, with the all-*trans* fraction falling below 50%.[13] In animal and human prostate tissue, the all-*trans* content falls even further, from 12% to 21% of the total lycopene content in normal human and malignant prostate tissue.[13–15] 5-*cis*-lycopene and 5-*cis*-lycophyll are particularly stable thermodynamically, are readily formed after chemical synthesis;[16–18] one is also found in abundance in vivo in both animal and human prostate (i.e., 5-*cis*-lycopene).[9,13] Whether the proportional tissue-specific differences in *cis*/*trans* isomer concentrations are attributable to differential absorption, concentrative uptake, or metabolic differences among tissues is not well understood; the intriguing possibility also exists that these geometric isomers are formed in vivo following interaction with reactive oxygen.[19,20]

A considerable body of evidence has accumulated demonstrating the inhibitory effect of lycopene on the growth of prostate and other cancer cell lines.[9,10,21] The biochemical mechanisms underlying the inhibitory effects of lycopene on the growth of cancer cells appear to be multi-factorial.[19] Documented mechanisms of lycopene action include: (1) antioxidant function (singlet oxygen quenching/radical chain breaking), recently verified in human target tissue as a reduction in 8-hydroxy-2′-deoxyguanosine (8-OHdG) levels after whole-food lycopene intervention;[7,19,22] (2) inhibition of cell cycle progression; (3) induction of apoptosis; (4) modulation of gap-junctional intercellular communication (GJIC) and connexin 43 (Cx43) levels; (5) inhibition of IGF-1 signal transduction; (6) inhibition of IL-6 expression; (7) induction of Phase II detoxifying enzymes; and (8) inhibition of androgen activation and signaling. Recently, bioactive in vivo lycopene oxidation products have been shown capable of induction of in vitro apoptosis of cancer cells, as well as enhancement of GJIC,[23–26] suggesting that studies of mechanism should be extended to these oxidative metabolites.

Epidemiology and whole-animal experiments have also repeatedly suggested a link between fat type and content in the diet and the risk of metastatic prostate cancer.[27] The mechanistic rationale for this dietary link has been established in human prostate cancer cell lines (e.g., the androgen-responsive LNCaP line), indicating potent roles for arachidonic acid and its oxidative metabolites 5-HETE (5-*S*-hydroxy-6,8,11,14-eicosatetraenoic acid) and 5-oxo-EET (5-*S*-oxo-6,8,11,14-eicosatetraenoic acid) in prostate cancer growth and metastasis.[28–31] The metabolism of arachidonic acid (AA) by either the cyclooxygenase (COX) or the lipoxygenase (LOX) pathway generates eicosanoids, which have been implicated in the pathogenesis of a variety of human diseases including cancer, and are significantly involved in tumor promotion, progression, and metastasis.[32,33] Aberrant expression of 5-, 12-, and 15-lipoxygenase in prostate cancer cells has been well documented and appears to contribute significantly to cellular proliferation.[34,35] The properties of 5-HETE in particular have identified it as a factor potentially capable of promoting survival of prostate cancer cells following androgen withdrawal and supporting tumor growth in the absence of androgen (i.e., an 'escape' or 'survival factor'). Thus, the development of 5-LOX inhibitors capable of interrupting the 5-lipoxygenase axis in prostate cancer cells remains the focus of numerous investigations, and there is increasing evidence suggesting that LOX inhibition is a promising therapeutic approach in the treatment of prostate cancer.[35,36]

Compounds with strong antioxidant and free radical scavenging properties, such as lycopene, may be effective in modulating LOX activity. In vitro, lycopene is a substrate of soybean LOX. The presence of this enzyme also significantly increased the production of lycopene oxidative metabolites.[37,38] The homology amongst plant and mammalian LOX enzymes is limited, however, sufficient conservation of important functional domains is found for predictive value.[39] No information is available on the biological activity of the tomato xanthophyll lycophyll.[17,18] Therefore, to obtain insight into additional molecular mechanisms by which lycopene and lycophyll and their oxidative metabolites might exert prominent anti-cancer effects, lycopene (ψ,ψ-carotene; all-*trans* and 5-*cis* isomers), its natural dihydroxy analog lycophyll (all-*trans*-ψ,ψ-carotene-16,16′-diol), and two non-enzymatically produced lycopene oxidation products (4-methyl-8-oxo-2,4,6-nonatrienal and 2,7,11-trimethyl-tetradeca-hexaene-1,14-dial; Fig. 1) were subjected to docking calculations with human 5-LOX. As no X-ray crystallography (XRC) structure for human 5-LOX has been published, a predictive 3D model was constructed through homology modeling based on the crystal structures of rabbit reticulocyte 15-LOX and of coral 8*R*-LOX. The model was found to accurately predict the binding energies of carotenoids to 5-LOX published previously.[39] The intact tomato carotenoids were found to bind with high affinity to a putative allosteric site on the 5-LOX enzyme (the 'cleavage site'), while their potential oxidative metabolites were capable of high-affinity direct competitive binding at the 5-LOX

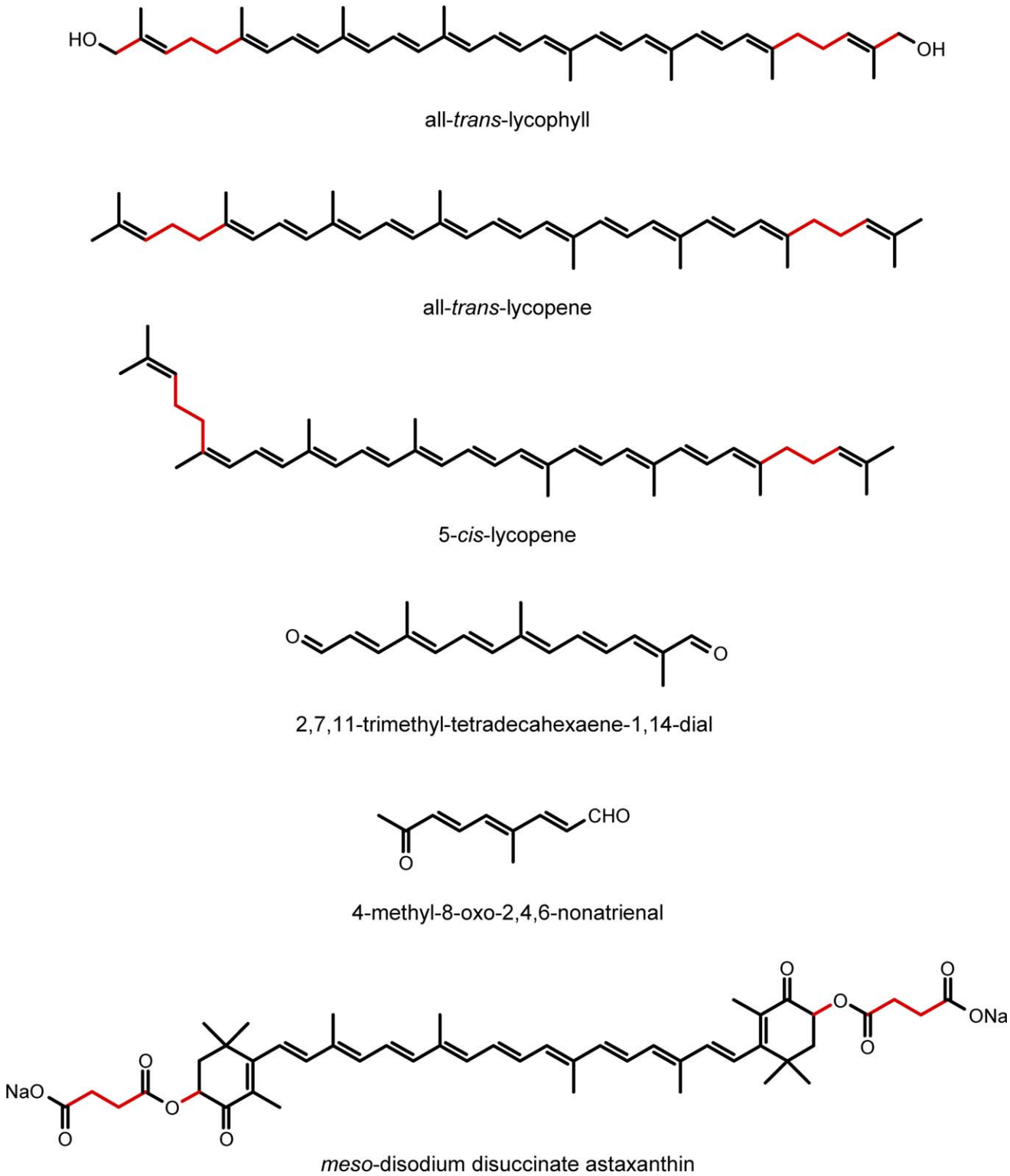


**Figure 1.** Chemical structures of the investigated tomato carotenoid ligands and associated oxidative metabolites. *Meso*-Cardax™ (*meso*-dAST; *meso*-disodium disuccinate astaxanthin) is included for relevant modeling/association constant calculations from previous work with 5-LOX, see text.[39] Rotatable bonds are shown in red.

active (catalytic) site. Therefore, the molecular modeling methods developed in seminal studies have been successfully applied in the current study to obtain predictive information for directing experimental studies on the molecular basis of pharmacologic ligand/LOX interactions.[39–41]

## 2. Results

### 2.1. Homology modeling

Lipoxygenases catalyze the peroxidation of diene-containing fatty acids and belong to a class of non-heme

iron metalloenzymes found in both plants and mammals. There are three major mammalian isozymes (5-LOX, 12-LOX, and 15-LOX) which oxygenate arachidonic acid at stereospecific carbon centers. Several crystallographically-determined structures of animal and plant lipoxygenases have been reported, showing a common overall folding pattern and very similar catalytic sites. 5-LOX is a monomeric enzyme constituting a single, 673 amino acid polypeptide chain folded into a two-domain structure.[42] The large C-terminal domain is the catalytic subunit, containing the catalytically active non-heme iron and the U-shaped hydrophobic substrate-binding pocket.[43] The N-terminal β-barrel domain (~110 residues) has been implicated in the binding of the enzyme to biomembranes.[44] Since no X-ray coordinates are currently available for human 5-LOX, different homology models were constructed. The first (Model S) was based on the crystal structure of 8*R*-lipoxygenase (PDB code: 2FNQ) sharing 38% sequence identity with 5-LOX. Furthermore, a chimeric model was built using both 8*R*-lipoxygenase and rabbit reticulocyte 15-LOX (sharing 37% sequence identity with 5-LOX; PDB code: 1LOX) as templates (Model M). A model based on a single 15-LOX template was not constructed, since there is a relatively long surface region (residues 176–188) missing in the experimental structure. More than 88% and 85% of the residues were in the 'core' regions of the Ramachandran plot in Models M and S, respectively (Table 1). Comparing the equilibrated and minimized final 15-LOX models with Procheck revealed that the model based on multiple templates (Model M) was of better quality than the model based on a single template (Model S). Therefore, the homology Model M was used in further docking calculations.

## 2.2. Validation of the 5-LOX homology model

The association constants of *meso*-disodium disuccinate astaxanthin ('*meso*-dAST;' *meso*-Cardax™) with 5-LOX were estimated in our previous study from spectroscopic data.[39] Therefore, comparison of the calculated (from the docked *meso*-dAST—5-LOX complex) and experimental binding energy of *meso*-Cardax™ to 5-LOX yielded information about the precision of the homology model for predicting the binding energies of other ligands under study. The experimental binding energy was derived from the association constant ($8 \times 10^5\ M^{-1}$) of the binding of the first *meso*-dAST molecule to 5-LOX published previously.[39] The calculated (−11.0 kcal/mol) and experimental binding energy values (−8.1 kcal/mol) were in reasonable agreement, indicating that the derived homology model could be used to reliably predict additional carotenoid ligand binding energies to 5-LOX.

**Table 1.** The quality of two homology models of 5-LOX (using one or more LOX structures as template(s))

| | Core | Allow | Gener | Disall |
|---|---|---|---|---|
| Model S | 85.1 | 11.2 | 2.6 | 1.0 |
| Model M | 88.3 | 10.2 | 0.7 | 0.8 |

Percentage of the amino acid residues in the different regions of the Ramachandran plot calculated by Procheck. Model S indicates the homology model built using 2FNQ as a template, Model M indicates the homology model built using 2FNQ and 1LOX as templates. Model M was utilized for subsequent calculations due to higher performance (see text). Gener and Disall mean residues in the generally allowed and disallowed regions, respectively.

## 2.3. Docking calculations

**2.3.1. Blind docking.** Molecular docking is the most common technique for the calculation of protein–ligand interactions. 'Blind docking' can successfully predict the possible ligand binding sites on the whole protein target.[45] This method is used in cases when (1) the binding site of the protein is not known, and (2) other sites besides the known catalytic site(s) are assumed to influence the enzymatic activity (i.e., allosteric mechanisms). Blind docking of lycopene and lycophyll to 5-LOX (Fig. 2) yielded different results than those obtained for the oxidative metabolites (Fig. 3). Blind docking of the intact tomato carotenoids resulted in the best docking energy at the 'cleavage site' (the putative allosteric site), while first rank docking positions of 4-methyl-8-oxo-2,4,6-nonatrienal and 2,7,11-trimethyl-tetradecahexaene-1,14-dial lay close to the catalytic site. The lack of polar end-groups in the case of lycopene (i.e., hydroxyls in all-*trans* configuration), as compared to lycophyll, did not influence the binding or the binding energies. Distraction of the linear shape of the lycopene ligand by introduction of a peripheral *cis* bond (5-*cis*-lycopene) led to decreased preference to the cleavage site (decreased binding energy), and preferred docking to other surface sites.

**2.3.2. Voidoo calculations.** Blind docking calculations are most useful for finding binding sites at the surface of protein targets. Although oxidative metabolites of lycopene were found to bind inside the protein structure with blind docking calculations, some 'buried' binding sites can be invisible using the blind docking method.

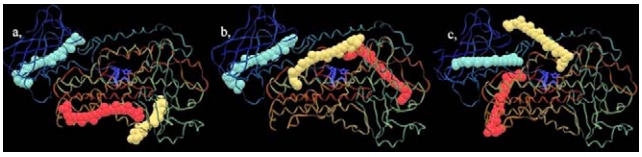


**Figure 2.** Three best-energy results of blind docking calculations: (a) lycophyll; (b) lycopene; (c) 5-*cis*-lycopene. Rank order from lower to higher energies: green, yellow, red.

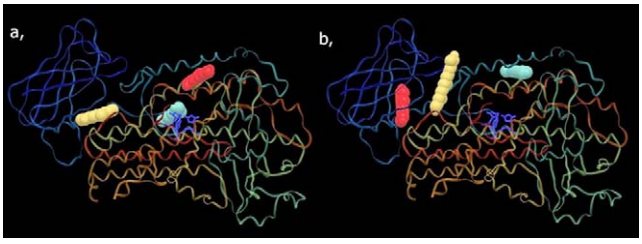


**Figure 3.** Three best-energy results of blind docking calculations: (a) 4-methyl-8-oxo-2,4,6-nonatrienal; (b) 2,7,11-trimethyl-tetradecahexaene-1,14-dial. Rank order from lower to higher energies: green, yellow, red.

Therefore, cavity calculations were carried out in order to identify cavities inside the protein. Four overlapping cavities were found, all of them located near the known catalytic site (data not shown). There were cavities identified on both sides of the catalytic center; the sum of the cavity volumes would enable the binding of smaller carotenoids inside the protein structure. However, it was unlikely that the wall-forming catalytic residues could suffer such drastic conformational change that these cavities would fuse into a larger one. The volume of the individual cavities did not allow accommodation of an intact, rigid, and linear acyclic C40 carotenoid. In contrast, the shorter metabolites (Fig. 1) had suitable molecular volume enabling binding to these pockets. Therefore, only the oxidative metabolites of lycopene were investigated in detail with focused docking at the catalytic site (carotenoids were docked with 'infinite' energy to the catalytic site; data not shown). Focused docking calculations for the catalytic site were performed using a simulation box, which included all four cavities found by Voidoo.

**2.3.3. Focused docking.** Focused docking calculations were carried out on the best energy sites revealed by blind docking calculations: (1) carotenoids were docked to the cleavage site identified by blind docking; (2) oxidative metabolites were docked to the buried sites revealed by blind docking calculations and identified by Voidoo calculations (catalytic site). All investigated ligands were found to be able to bind to the cleavage site with good energy values (data not shown). The long linear groove at the interface of the N- and C-terminal domains of 5-LOX renders the rigid, 'stick-like' carotenoids ideal ligands for this site (Fig. 4). The shape of both all-*trans*-lycophyll and all-*trans*-lycopene fits almost exactly to the cleft formed by the surface residues at this site. Besides the hydrophobic residues (Val109, Val110, and Leu603), there are numerous hydrophilic and charged residues near the polyene chain. The hydroxyl (OH) groups of lycophyll were fixed in the cleft and formed hydrogen bonds with Q129, K161, and D162, respectively.

The absolute molecular length of the investigated carotenoids (about 30 Å) hindered their binding to the catalytic site in both *trans* and *cis* conformations. The lycopene metabolite 4-methyl-8-oxo-2,4,6-nonatrienal was docked directly to the catalytic site, near the iron-coordinating histidine residues (Fig. 5). The molecule formed numerous hydrophobic contacts at the binding site, namely with Ile406 and Ile415, Leu368, Leu414, and Leu606, and Ala410. Pi–pi (π–π) interactions of the conjugated chain with histidines and Phe421 may strengthen the ligand binding. The aldehyde group of the metabolite points toward the polar part of the pocket, and was within interaction distance (<4 Å) of Gln363, Thr364, and Gln557.

2,7,11-Trimethyl-tetradecahexaene-1,14-dial (the dial metabolite) was also capable of binding directly to the catalytic site despite its increased size relative to the shorter oxidative metabolite (Fig. 6). As compared to the shorter metabolite, it established additional hydrophobic (Ala424, Ala603) and π–π interactions (Phe151, Phe359). The hydrophobic residues that could interact with the nonatrienal metabolite were also in close proximity to the dial metabolite. The ketone end groups were in suitable positions to form intermolecular H-bonds with Ser154 and Asn425, respectively.

## 2.4. Calculation of the binding energies

It was anticipated that each ligand would bind to the site defined by blind docking with the greatest affinity. The intact tomato carotenoids bound to the cleavage site (as their absolute molecular volume would not allow binding to the catalytic site), while the oxidative

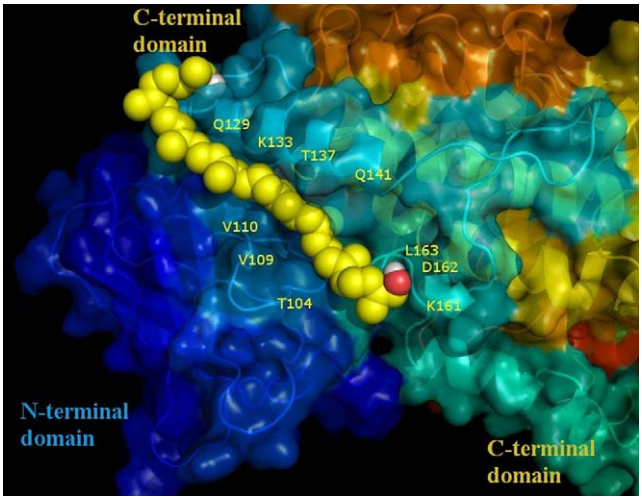


**Figure 4.** Calculated model of all-*trans*-lycophyll binding to 5-LOX. The interface of the N-terminal and C-terminal domains has a long linear cleft, ideally shaped for 'stick-like' carotenoid molecules in all-*trans* configuration. Residues within 4 Å of the bound ligand are indicated (within 'interaction distance').

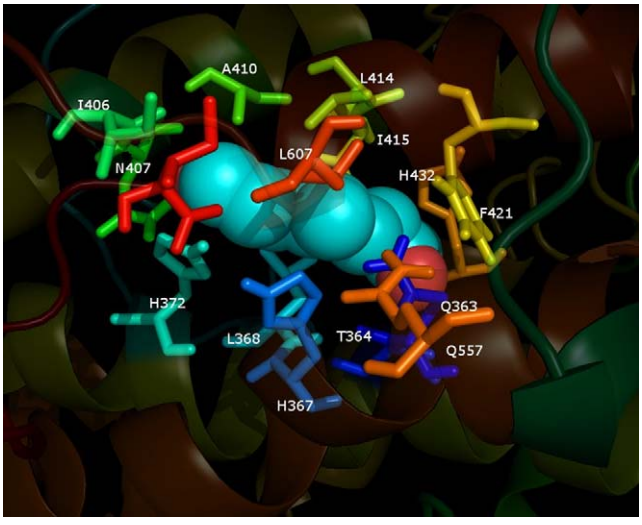


**Figure 5.** Calculated model of interaction of 4-methyl-8-oxo-2,4,6-nonatrienal with 5-LOX. The ligand molecule fits into the catalytic site of 5-LOX, forming hydrophobic interactions with leucines, isoleucines, and histidines. The amino acid residues within 4 Å distance of the docked ligand are indicated ('interaction distance').

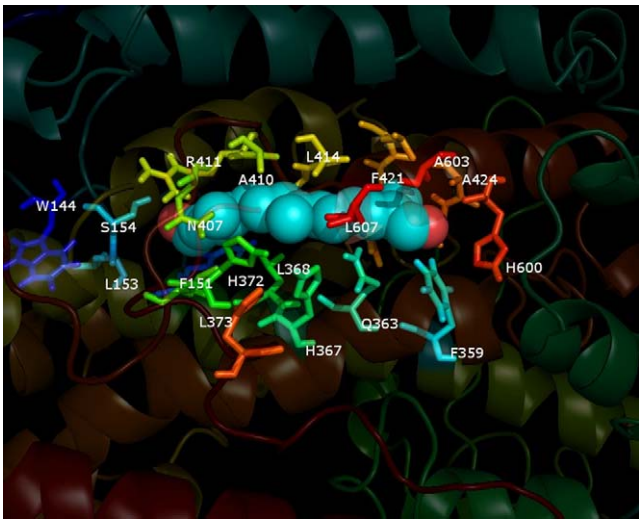


**Figure 6.** Calculated model of 2,7,11-trimethyl-tetradecahexaene-1,14-dial binding to 5-LOX. After a short MD simulation, the ligand binds with high affinity to the catalytic site. The amino acid residues within 4 Å distance of the docked ligand are indicated ('interaction distance').

metabolites favored binding to the catalytic site. Therefore, the best focused docking results were subject to an energy minimization procedure using the Gromacs MD method to relax conformations obtained from Autodock. In this manner, a better estimate of the binding energy was achieved. Table 2 shows the calculated intermolecular interaction energies after a short MD relaxation of the best energy complex models. The relatively large size of metabolite 2,7,11-trimethyl-tetradecahexaene-1,14-dial caused a high calculated interaction energy (−2.60 kcal/mol) before MD simulations, but after allowing side-chain flexibility, a very low calculated docking energy resulted (Table 2). This finding in particular substantiated the usefulness of the MD methods. It has been reported that the substrate binding cavity of the 5-LOXs is about 20% larger than that of the 15-LOXs.[46] Without using MD, the smaller catalytic pocket of the 5-LOX homology model generated by the X-ray data for 15-LOX would not be able to accommodate the dial metabolite, and therefore potentially yielding a false negative result.

## 3. Discussion

In the current study, the binding of lycophyll, all-*trans* and 5-*cis*-lycopene, and several autooxidative metabolites to human 5-LOX was investigated with molecular modeling methods. Two different mechanisms for modulation of 5-LOX enzyme activity have been described: (1) the competitive pathway, by means of the direct binding of a ligand molecule to the active center (catalytic site); and (2) the reduction of lipid peroxidation via radical-chain breaking activity, which does not require direct interaction with the enzyme to occur (i.e., modulation of redox state and tone). In addition, regulatory activity by the β-barrel domain for LOX catalytic activity has been suggested by several authors. β-barrel truncation of the rabbit 12/15-LOX results in impaired catalytic efficiency.[44] Similarly, the isolated catalytic domain of soybean LOX-1 exhibits an augmented catalytic activity compared with the native enzyme.[47] And most recently, a role for the N-terminal β-barrel has been proposed in LOX/substrate and/or LOX/product interactions.[48] The regulatory importance of the β-barrel might be connected with its conformational motion relative to the catalytic subunit, as demonstrated by small angle X-ray scattering.[42,49] Accordingly, small molecule binding at the interdomain cleft of LOX may affect the kinetics and other biochemical parameters of LOX enzymatic reactions in vivo (indirect allosteric protein effects).

As there was no available X-ray structure published for human 5-LOX, a homology model was constructed. The best available templates (8-LOX and 15-LOX) share practically an identical backbone structure according to published X-ray data. Generation of different models based on one or two templates will mostly change the side-chain conformations of the models. The 'validity' of the generated models can be evaluated from the following points of view: (1) how accurately the model's geometric properties fit with our general understanding of protein structure as it relates to function; and (2) how the different side-chain conformations result in different cavity and surface shapes and sizes with different ligand binding properties. Models often possess smaller ligand binding sites than the real structures. In models, 'random' side-chain conformations can result in residues occupying the available space of the pockets. Given this inherent limitation of modeling, models exhibiting larger cavities are more likely to be correct predictors for a given protein. Homology models based on both templates had higher general quality as revealed by Procheck, and larger cavities as revealed by Voidoo (data not shown). Thus, the model generated from multiple templates appeared to be a better representation of the real protein.

The seminal study that demonstrated that carotenoids could directly interact with the human 5-LOX enzyme

**Table 2.** Calculated intermolecular interaction energies after molecular dynamics (MD) relaxation of the best energy complex models

| Ligand | Intermolecular interaction energy after MD (kcal/mol) | Site |
|---|---|---|
| All-*trans*-lycophyll | −14.01 | Cleavage |
| All-*trans*-lycopene | −14.28 | Cleavage |
| 5-*cis*-Lycopene | −13.89 | Cleavage |
| 4-Methyl-8-oxo-2,4,6-nonatrienal | −7.13 | Catalytic |
| 2,7,11-Trimethyl-tetradecahexaene-1,14-dial | −11.85 | Catalytic |
| *meso*-Astaxanthin disodium disuccinate (Cardax™) | −11.03 | Cleavage |

also proposed a preliminary model of C40-carotenoid derivative binding to lipoxygenases.[39] A good correlation between the predicted binding free energy based on the current homology model and the experimental binding energy of Cardax™ to 5-LOX in the seminal study suggests that not only the geometry, but also the energy of the interaction can be predicted with reasonable quality.

Blind docking has proven to be a successful tool for a priori prediction of protein–ligand interactions. In our study, it was introduced for the detection of possible natural tomato carotenoid binding sites on the whole protein target. However, buried sites are often invisible for blind docking calculations, and therefore additional cavity calculations were performed to explore the available non-surface sites. It was anticipated that each ligand would bind to the site with the lowest calculated docking energy, defined by either the blind docking for the whole protein target, or by the focused docking at the buried sites. Our results showed that lycopene and lycophyll (in all-*trans* geometric form) bound to the 'cleavage site' of the enzyme, the unique long cleft situated between the N- and C-terminal domains. The end groups of the natural xanthophyll carotenoid lycophyll were found not to appreciably affect the overall binding energy relative to that of lycopene. The size (molecular length) of lycopene and lycophyll did not allow their binding to the catalytic site. Therefore, these results suggested three possible mechanisms by which the natural tomato carotenoids could modulate 5-LOX enzyme activity:

(1) Binding of all-*trans*-lycopene or -lycophyll into the cleft could modulate enzyme activity by an allosteric mechanism. The presence of an allosteric binding site in both soybean and human 15-LOX has been demonstrated experimentally.[50,51]
(2) Binding of a natural tomato carotenoid could affect the interdomain movement of the N-terminal and C-terminal domains, which has been shown to have functional importance for regulation of the catalytic activity.[42,49]
(3) Binding of natural tomato carotenoid molecule(s) in the cleavage site could place the carotenoids in reasonable proximity for trapping free radical intermediates generated during the enzyme–substrate reaction, or altering the ion state of the active center. Antioxidant activity in the vicinity of the activity center can result in the inhibition of LOX-catalyzed reactions.[52]

Blind docking of the autoxidative metabolites 4-methyl-8-oxo-2,4,6-nonatrienal and 2,7,11-trimethyl-tetradecahexaene-1,14-dial resulted in most favorable ('best-energy') results near or at the catalytic site, suggesting the potential direct competitive 5-LOX inhibitory effect of these compounds. According to our modeled complexes, the large number of van der Waals interactions between the surrounding lipophilic side chains together with the hydrogen (H)-bonding capabilities of the polar end groups fulfilled the typical structural requirements for a 5-LOX inhibitor.[43] This result is in good agreement with the reported inhibitory effect of 4-hydroxy-2(*E*)-nonenal on soybean LOX,[53] which is a chemically similar structural analog of the lycopene autooxidative product 4-methyl-8-oxo-2,4,6-nonatrienal found to bind with high-affinity to the catalytic site of our homology model. Additionally, the residues found to be involved in lycopene oxidative metabolite binding in our models were similar to those (Phe359, Ala424, Asn425, and Ala603) identified by independent mutational studies as critically involved side chains in the substrate binding of 5-LOX.[54]

Both 4-methyl-8-oxo-2,4,6-nonatrienal and 2,7,11-trimethyl-tetradecahexaene-1,14-dial were formed non-enzymatically from lycopene in vitro, using ozonolysis and hydrogen peroxide/osmium tetroxide, respectively.[23,25] Lycopene and lycophyll share the same chromophore, and oxidative cleavage sites in the polyene are likely shared between the two compounds due to the similarity in physicochemical structure.[2] The possibility therefore exists for the in vivo production of these compounds in areas of high oxidative stress and/or peroxide tone, for example, in human prostate cancer cells—particularly in the setting of chronic inflammation such as prostatitis.[28,55] Oxidative metabolites formed in vivo through an epoxide intermediate have previously been shown to have bioactivity, supporting this supposition.[26]

Recent advances in characterization of carotenoid cleavage enzymes may also provide clues to the possibility of enzymatic formation of active lycopene-series metabolites. Novel 9′,10′-dioxygenases have been added to the growing family of double bond cleavage enzymes characterized from plants and animals.[56] If an excentric dioxygenase is capable of utilizing lycophyll as well as lycopene as a substrate in vivo, then supplementation with either compound could produce direct enzyme inhibitory activity of the 5-LOX catalytic site through 'metabolic activation.' Such enzymes have already been identified in the tomato genome; they produce a symmetric C14 dial only slightly shorter than 2,7,11-trimethyl-tetradecahexaene-1,14-dial utilized in the current study.[57] Provocatively, oxidative metabolites of astaxanthin have been identified by HPLC in humans, which suggests the presence of such an excentric cleavage enzyme.[58] This information, coupled with the allosteric and antioxidant mechanisms for the intact parent tomato carotenoids described above, could prescribe significant therapeutic potential on the 5-LOX axis suggested in Section 1.

## 4. Conclusion

A homology model of 5-LOX was built using published X-ray structures of related lipoxygenases as templates. The model was found to reasonably predict the binding energies of other C40 carotenoids as revealed by the comparison of the measured and calculated binding energies of *meso*-Cardax™ to 5-LOX. Subsequently, the possible binding interactions with human 5-LOX of the prominent natural members of the

pharmacologically important tomato carotenoid family (lycopene, lycophyll) and several autoxidative metabolites were investigated for the first time. It was found that the cleft at the interface of the N-terminal and C-terminal domains of the protein had an ideal shape for intact parent carotenoid binding, particularly of the all-*trans* geometric forms. Allosteric conformational change of the 5-LOX enzyme may be possible based on this binding. Next, the autooxidative metabolites of lycopene were demonstrated to have high-affinity binding at or near the active (catalytic) site of the enzyme, suggesting potential for direct enzyme inhibition after supplementation of the parent compounds in vivo, particularly in tissues undergoing oxidative stress such as prostate. These predictive data can be utilized to direct experimental studies on the modulation of the important 5-LOX pathway in prostate cancer—and the generation of potent oxidative and pro-inflammatory mediators, such as the survival factor 5-HETE—in model systems and human clinical trials of these natural compounds.

## 5. Experimental

### 5.1. Amino acid sequence alignment and homology modeling

The initial sequence alignment of lipoxygenases was carried out using the ClustalW program.[59] The sequence alignment was refined and three-dimensional (3D) models comprising all non-hydrogen atoms were generated by the MODELLER6 package.[60] The package is based on a distance restraint algorithm—satisfying spatial constraints extracted from the alignment of the known protein(s), which is (are) the template structure(s)—with the target sequence and from the CHARMM-22 force field. A bundle of five (5) models from random generation of the starting structure was calculated. Subsequently, the best model was subjected to a short molecular dynamics (MD) refinement. MD calculations were carried out using the GROMACS program package.[61] The best homology model was relaxed for 100 ps in order to obtain equilibrium. The tertiary structure models were checked using Procheck.[62] Two homology models were built using the following structures as templates: (1) structure of 8-LOX (PDB code: 2FNQ;[63] Model S) and (2) a chimeric model using 8-LOX and 15-LOX as templates (PDB codes 2FNQ, 1LOX;[46,63] Model M).

### 5.2. Blind docking calculations

The MMFF94 force field[64] with conjugate gradient method was used for energy minimization of the investigated ligands (Fig. 1). Gasteiger partial charges were added to the ligand atoms. Non-polar hydrogen atoms were merged, and rotatable bonds were defined with the aid of Autodock tools (Fig. 1).[65]

Blind docking calculations were carried out on the homology model based on multiple templates (Model M). Essential hydrogen atoms, Kollman united atom type charges, and solvation parameters were added with the aid of AutoDock tools.[65] Affinity (grid) maps of $150 \times 150 \times 200$ grid points and 0.500 Å spacing were generated using the Autogrid program,[65] and maps were centered on the protein center. AutoDock parameter set- and distance-dependent dielectric functions were used in the calculation of the van der Waals and the electrostatic terms, respectively. All rotatable torsions (Fig. 1) were released during docking. Each docking experiment was derived from 100 different runs that were set to terminate after a maximum of 1,500,000 energy evaluations. During the search, a translational step of 0.2 Å, and quaternion and torsion steps of 5 were applied. Root mean squared deviation (RMSD) was calculated for the resulting 100 structures using ligand structures of minimum energies at each job as references. A 2.0 Å tolerance was used to form clusters of the closest structures.

### 5.3. Focused docking

Refined complex structures were calculated corresponding to the cleavage site and the catalytic site. Smaller grid maps, namely 100 grid points in each Cartesian direction, and 0.375 Å spacing were generated using the Autogrid program. The other parameters were the same as were described for the blind docking calculations.

### 5.4. Voidoo calculations

The program Voidoo (Uppsala Software Factory; USF, Uppsala, Sweden) was used to identify binding cavities and to calculate cavity volumes for 5-LOX. This program can be used to detect unknown cavities or to delineate known cavities, either of which may be connected to the outside of the molecule or molecular assembly under study.[66]

### 5.5. Binding energy calculations

MD calculations were carried out on the lowest energy complexes. The GROMACS program package[61] was applied for generation of a simulation box, addition of explicit water molecules and counter ions. Complexes were energy minimized using the GROMOS force field[67] implemented in the program package. Short 0.1 ps long unrestrained MD simulations were performed to equilibrate the surrounding molecules and to generate conformations for calculations of intermolecular interaction energy using Autodock.

## Acknowledgments

The authors thank Dave M. Watumull for bibliographic assistance and formatting of the final manuscript. Henry L. Jackson, Ph.D., provided background literature on state-of-the-art in carotenoid cleavage enzyme characterization.

## References and notes

1. Delgado-Vargas, F.; Jimenez, A. R.; Paredes-Lopez, O. *Crit. Rev. Food Sci. Nutr.* **2000**, *40*, 173.

2. Britton, G., Liaaen-Jensen, S., Pfander, H., Mercadante, A. Z. Egeland, E. S., Eds.; *Carotenoids Handbook*; Birkhäuser: Basel, 2004.
3. Di Mascio, P.; Kaiser, S.; Sies, H. *Arch. Biochem. Biophys.* **1989**, *274*, 532.
4. Clinton, S. K. *Nutr. Rev.* **1998**, *56*, 35.
5. Stahl, W.; Sies, H. *Biochim. Biophys. Acta* **2005**, *1740*, 101.
6. Tapiero, H.; Townsend, D. M.; Tew, K. D. *Biomed. Pharmacother.* **2004**, *58*, 100.
7. Chen, L.; Stacewicz-Sapuntzakis, M.; Duncan, C.; Sharifi, R.; Ghosh, L.; van Breemen, R.; Ashton, D.; Bowen, P. E. *J. Natl. Cancer Inst.* **2001**, *93*, 1872.
8. Kucuk, O.; Sarkar, F. H.; Sakr, W.; Djuric, Z.; Pollak, M. N.; Khachik, F.; Li, Y. W.; Banerjee, M.; Grignon, D.; Bertram, J. S.; Crissman, J. D.; Pontes, E. J.; Wood, D. P., Jr. *Cancer Epidemiol. Biomarkers Prev.* **2001**, *10*, 861.
9. Limpens, J.; Schroder, F. H.; de Ridder, C. M.; Bolder, C. A.; Wildhagen, M. F.; Obermuller-Jevic, U. C.; Kramer, K.; van Weerden, W. M. *J. Nutr.* **2006**, *136*, 1287.
10. Bhuvaneswari, V.; Nagini, S. *Curr. Med. Chem. Anti-cancer Agents* **2005**, *5*, 627.
11. Khachik, F.; Carvalho, L.; Bernstein, P. S.; Muir, G. J.; Zhao, D. Y.; Katz, N. B. *Exp. Biol. Med. (Maywood)* **2002**, *227*, 845.
12. Rissanen, T.; Voutilainen, S.; Nyyssonen, K.; Salonen, J. T. *Exp. Biol. Med. (Maywood)* **2002**, *227*, 900.
13. Clinton, S. K.; Emenhiser, C.; Schwartz, S. J.; Bostwick, D. G.; Williams, A. W.; Moore, B. J.; Erdman, J. W., Jr. *Cancer Epidemiol. Biomarkers Prev.* **1996**, *5*, 823.
14. Stahl, W.; Sies, H. *Arch. Biochem. Biophys.* **1996**, *336*, 1.
15. van Breemen, R. B.; Xu, X.; Viana, M. A.; Chen, L.; Stacewicz-Sapuntzakis, M.; Duncan, C.; Bowen, P. E.; Sharifi, R. *J. Agric. Food Chem.* **2002**, *50*, 2214.
16. Ernst, H. *Pure Appl. Chem.* **2002**, *74*, 2213.
17. Jackson, H. L.; Nadolski, G. T.; Braun, C.; Lockwood, S. F. *Org. Process. Res. Dev.* **2005**, *9*, 830.
18. Braun, C. L.; Jackson, H. L.; Lockwood, S. F.; Nadolski, G. *J. Chromatogr., B* **2006**, *834*, 208.
19. Wertz, K.; Siler, U.; Goralczyk, R. *Arch. Biochem. Biophys.* **2004**, *430*, 127.
20. Stahl, W.; Sies, H. *Ann. N.Y. Acad. Sci.* **1993**, *691*, 10.
21. Guns, E. S.; Cowell, S. P. *Nat. Clin. Pract. Urol.* **2005**, *2*, 38.
22. Everson, K. M.; McQueen, C. E. *Am. J. Health. Syst. Pharm.* **2004**, *61*, 1562.
23. Zhang, H.; Kotake-Nara, E.; Ono, H.; Nagao, A. *Free Radic. Biol. Med.* **2003**, *35*, 1653.
24. Nara, E.; Hayashi, H.; Kotake, M.; Miyashita, K.; Nagao, A. *Nutr. Cancer* **2001**, *39*, 273.
25. Aust, O.; Ale-Agha, N.; Zhang, L.; Wollersen, H.; Sies, H.; Stahl, W. *Food Chem. Toxicol.* **2003**, *41*, 1399.
26. Bertram, J. S.; King, T.; Fukishima, L.; Khachik, F. In *Antioxidant and Redox Regulation of Genes*; Sen, C. K., Sies, H., Baeuerle, P. A., Eds.; Academic Press: San Diego, CA, 2000; pp 409–424.
27. Sonn, G. A.; Aronson, W.; Litwin, M. S. *Prostate Cancer Prostatic Dis.* **2005**, *8*, 304.
28. Ghosh, J.; Myers, C. E. *Proc. Natl. Acad. Sci. U.S.A.* **1998**, *95*, 13182.
29. Myers, C. E.; Ghosh, J. *Eur. Urol.* **1999**, *35*, 395.
30. Ghosh, J. *Biochem. Biophys. Res. Commun.* **2003**, *307*, 342.
31. McCarty, M. F. *Integr. Cancer. Ther.* **2004**, *3*, 349.
32. Catalano, A.; Procopio, A. *Histol. Histopathol.* **2005**, *20*, 969.
33. Claria, J.; Romano, M. *Curr. Pharm. Des.* **2005**, *11*, 3431.
34. Kelavkar, U.; Lin, Y.; Landsittel, D.; Chandran, U.; Dhir, R. *J. Carcinog.* **2006**, *5*, 9.
35. Matsuyama, M.; Yoshimura, R.; Mitsuhashi, M.; Hase, T.; Tsuchida, K.; Takemoto, Y.; Kawahito, Y.; Sano, H.; Nakatani, T. *Int. J. Oncol.* **2004**, *24*, 821.
36. Yoshimura, R.; Matsuyama, M.; Kuratsukuri, K.; Tsuchida, K.; Takemoto, Y.; Nakatani, T. *Drugs Future* **2005**, *30*, 351.
37. dos Anjos Ferreira, A. L.; Yeum, K. J.; Russell, R. M.; Krinsky, N. I.; Tang, G. *J. Nutr. Biochem.* **2004**, *15*, 493.
38. Biacs, P. A.; Daood, H. G. *Biochem. Soc. Trans.* **2000**, *28*, 839.
39. Lockwood, S. F.; Penn, M. S.; Hazen, S. L.; Bikádi, Z.; Zsila, F. *Life Sci.* **2006**, *79*, 162, and references therein.
40. Kenyon, V.; Chorny, I.; Carvajal, W. J.; Holman, T. R.; Jacobson, M. P. *J. Med. Chem.* **2006**, *49*, 1356.
41. Bindu, P. H.; Sastry, G. M.; Sastry, G. N. *Biochem. Biophys. Res. Commun.* **2004**, *320*, 461.
42. Kühn, H.; Saam, J.; Eibach, S.; Holzhutter, H. G.; Ivanov, I.; Walther, M. *Biochem. Biophys. Res. Commun.* **2005**, *338*, 93.
43. Du, L.; Zhang, Z.; Luo, X.; Chen, K.; Shen, X.; Jiang, H. *J. Biochem. (Tokyo)* **2006**, *139*, 715.
44. Walther, M.; Anton, M.; Wiedmann, M.; Fletterick, R.; Kuhn, H. *J. Biol. Chem.* **2002**, *277*, 27360.
45. Hetényi, C.; van der Spoel, D. *Protein Sci.* **2002**, *11*, 1729.
46. Gillmor, S. A.; Villasenor, A.; Fletterick, R.; Sigal, E.; Browner, M. F. *Nat. Struct. Biol.* **1997**, *4*, 1003.
47. Maccarrone, M.; Salucci, M. L.; van Zadelhoff, G.; Malatesta, F.; Veldink, G.; Vliegenthart, J. F.; Finazzi-Agro, A. *Biochemistry* **2001**, *40*, 6819.
48. Romanov, S.; Wiesner, R.; Myagkova, G.; Kuhn, H.; Ivanov, I. *Biochemistry* **2006**, *45*, 3554.
49. Hammel, M.; Walther, M.; Prassl, R.; Kuhn, H. *J. Mol. Biol.* **2004**, *343*, 917.
50. Mogul, R.; Johansen, E.; Holman, T. R. *Biochemistry* **2000**, *39*, 4801.
51. Ruddat, V. C.; Whitman, S.; Holman, T. R.; Bernasconi, C. F. *Biochemistry* **2003**, *42*, 4172.
52. Serpen, A.; Gokmen, V. *J. Sci. Food Agric.* **2006**, *86*, 401.
53. Gardner, H. W.; Deighton, N. *Lipids* **2001**, *36*, 623.
54. Schwarz, K.; Walther, M.; Anton, M.; Gerth, C.; Feussner, I.; Kuhn, H. *J. Biol. Chem.* **2001**, *276*, 773.
55. Shen, Z.; Wu, W.; Hazen, S. L. *Biochemistry* **2000**, *39*, 5474.
56. Wyss, A. *J. Nutr.* **2004**, *134*, 246S.
57. Simkin, A. J.; Schwartz, S. H.; Auldridge, M.; Taylor, M. G.; Klee, H. J. *Plant J.* **2004**, *40*, 882.
58. Kistler, A.; Liechti, H.; Pichard, L.; Wolz, E.; Oesterhelt, G.; Hayes, A.; Maurel, P. *Arch. Toxicol.* **2002**, *75*, 665.
59. Thompson, J. D.; Higgins, D. G.; Gibson, T. J. *Nucleic Acids Res.* **1994**, *22*, 4673.
60. Sali, A.; Blundell, T. L. *J. Mol. Biol.* **1993**, *234*, 779.
61. Berendsen, H. J. C.; van der Spoel, D.; van Drunen, R. *Comput. Phys. Commun.* **1995**, *91*, 43.
62. Laskowski, R. A.; MacArthur, M. W.; Moss, D. S.; Thornton, J. M. *J. Appl. Crystallogr.* **1993**, *26*, 283.
63. Oldham, M. L.; Brash, A. R.; Newcomer, M. E. *J. Biol. Chem.* **2005**, *280*, 39545.
64. Halgren, T. A. *J. Am. Chem. Soc.* **1992**, *114*, 7827.
65. Morris, G. M.; Goodsell, D. S.; Halliday, R. S.; Huey, R.; Hart, W. E.; Belew, R. K.; Olson, A. J. *J. Comput. Chem.* **1998**, *19*, 1639.
66. Kleywegt, G. J.; Jones, T. A. *Acta Crystallogr., Sect. D* **1994**, *50*, 178.
67. Hermans, J.; Berendsen, H. J. C.; Van Gunsteren, W. F.; Postma, J. P. M. *Biopolymers* **1984**, *23*, 1513.